rhd instruments
flexible cell solutions

# Application note

## Cathode Active Material Stress/Strain Behaviour and Electronic/Ionic Conductivity

02/2026
Christoffer Folkers-Karlsson
rhd instruments GmbH & Co. KG

# Introduction

The mechanical properties of lithium-ion battery active materials are crucial for their successful application in electrodes [1]. Their compressibility under applied pressure is important not only for processability during electrode fabrication and calendering, but also for sustained electrochemical performance throughout the battery's lifetime [1, 2]. A main pathway for capacity loss of cathode active materials (CAMs) such as $LiNi_{1-x-y}Mn_xCo_yO_2$ (NMC) is particle cracking due to mechanical stress developed during cycling [2].

Furthermore, active materials are mixed conductors, requiring both electronic and ionic conductivity to function in the battery. Accurate determination of these two types of conductivity is a vital part of material optimization, and they also have a large pressure and temperature dependence [3]. However, these measurements are often impeded by the fact that the sample thickness is difficult to determine accurately under an applied load.

In this application note, the mechanical and electrical properties of two pristine CAM samples were investigated. Specifically, the pressure-dependent density during and after powder compaction was monitored using linear variable differential transformer (LVDT) sensors, yielding stress/strain curves of the powder and pressed pellets. The ionic and electronic conductivities could be distinguished at different pressures and temperatures by electrochemical impedance spectroscopy (EIS). The *in-situ* thickness information was key to obtaining correct conductivity values, rather than relying on a thickness measured *ex situ* without applied force.

# Experimental

Two CAM samples comprised of surface coated high-nickel-content NMC (BASF SE) were studied in their pristine state in this application note: Polycrystalline $LiNi_{0.85}Mn_{0.05}Co_{0.10}O_2$ (NMC-PC) and single crystal $LiNi_{0.83}Mn_{0.05}Co_{0.12}O_2$ (NMC-SC) powder. The samples had similar particle sizes ($d_{50}$ = 3.8 µm) and tap densities (2.19 and 2.09 g/cm$^3$ for NMC-PC and NMC-SC, respectively).

A CompreCell 6C [4] was filled with pure CAM (400 mg/cm$^2$) in a glove box, resulting in about 1.7 mm sample thickness of powder. In this cell, the sample is constrained in an $Al_2O_3$ sleeve (6 mm sample diameter) and pressed between two hard metal (tungsten carbide) pistons. The total cell height was measured with a height gauge before mounting the LVDT Distance Add-on [5] (see picture on title page) for sample thickness monitoring, using the *ex-situ* measured cell height as the tare value before pressure application. The pressure and temperature were applied to the sample by a CompreDrive [6] with an HC Add-on [7]. EIS was performed at 1 MHz – 10 mHz (10 mV rms amplitude) at each pressure and temperature setpoint using a NEISYS (Novocontrol Technologies GmbH & Co. KG). A load/short calibration

was performed beforehand using either gold foil or a 100 Ω resistor in the CompreCell. No significant temperature dependence of the resistance contribution from the CompreCell itself was found.

First, the sample was compressed at increasing pressure steps from 10 MPa to 1.7 GPa at 25 °C, followed by a stepped pressure decrease to 10 MPa. This pressure cycle was performed a total of three times, before performing one temperature cycle between -30 °C and 100 °C at 200 MPa. Finally, a pressure cycle (as above) was performed at -30 °C. An equilibration time of 1 hour at each temperature, and 5 minutes at each pressure, was applied to ensure stable measurement conditions. The control of pressure, temperature, and electrochemical measurements, as well as collecting all data including sample thickness, was done with a procedure running in CompreDriveControl 1.17 (rhd instruments GmbH & Co. KG).

Edelweiss 1.0 [8] was used for data analysis and for creating the plots in this application note, while RelaxIS 3.0 [9] was used for equivalent circuit fitting.

The **sample pellet thickness *h*** was measured *in situ* at each **pressure *p*** and **temperature *T***. Since the cell pistons also deform under pressure, the same procedure was performed with an empty cell to quantify the cell contribution to the total thickness change. This was then subtracted to obtain the sample thickness at each pressure and temperature:

$$h(p,T) = h_{cell+sample}(p,T) - h_{cell}(p,T)$$

Note that due to significant hysteresis between the pressure increase and decrease sweeps, it's important to follow the same pressure procedure for the sample as for the blank measurement and perform the correction for the corresponding values.

Knowing how the pellet thickness changes with pressure, we can calculate several mechanical properties of the sample such as the **pellet density ρ**, which is determined from the mass of sample ($m$), the cross-section area of the pellet ($A$), and $h$:

$$\rho(p) = \frac{m}{A \cdot h(p)}$$

The **engineering strain *e*** is defined as the change in pellet thickness relative to the initial value:

$$e(p) = \frac{h(p) - h_{initial}}{h_{initial}}$$

Since the pellet is under compressive load in this case, the strain is negative. Finally, the **conductivity *σ*** was calculated based on the resistance $R$ fitted from EIS, and the pellet thickness *at that pressure and temperature*:

$$\sigma(p,T) = \frac{1}{R(p,T)} \cdot \frac{h(p,T)}{A}$$

At a certain pressure, the conductivity is expected to follow the Arrhenius equation:

$$\sigma(T) = \sigma_0 \cdot e^{-\frac{E_a}{k_B T}}$$

where $E_a$ is the activation energy and $k_B$ is the Boltzmann constant. The **resistivity** is the reciprocal of the conductivity.

# Results and Discussion

The initial compaction of the CAM powders could be followed by monitoring the density increase to 3.99 g/cm³ (NMC-PC) and 4.45 g/cm³ (NMC-SC) as the pressure was increased to 1.7 GPa (**Figure 1**). At that point, the powder had been pressed into a pellet. The weak pressure dependence of the pellet density was measured during the pressure decrease.

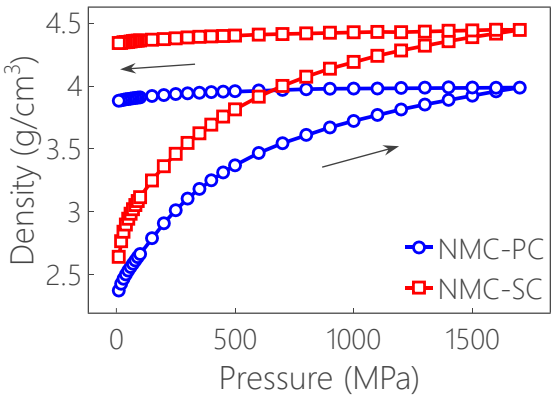


***Figure 1.*** *Density of powder (upwards sweep) and compacted pellet (downwards sweep).*

Another way to display the results of the powder compaction is as a stress/strain curve (**Figure 2**). The single crystal CAM was compressed more (46%) than the polycrystalline sample (42%), resulting in the higher pellet density despite similar tap densities. The stress/strain curve of the second pressure cycle corresponds to the deformation of the pressed pellets. Here, NMC-SC deformed slightly less (2.5%) than NMC-PC (3.3%).

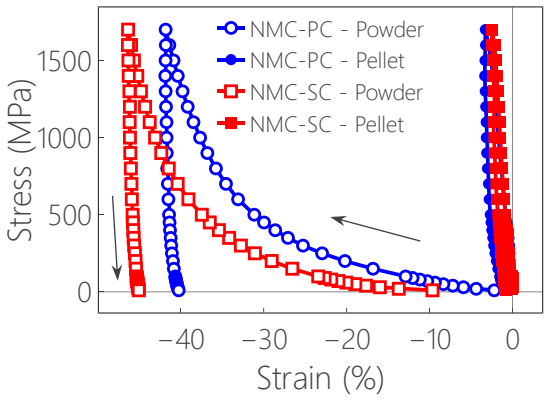


***Figure 2.*** *Stress/strain curves for the powder compaction (open symbols) and the pressed pellet (closed symbols).*

The impedance spectra of the pressed NMC-PC pellet showed almost perfect resistive behaviour, with some inductance visible at the highest frequencies (**Figure 3a**). This is consistent with the electronic conductivity of the CAM, since the pistons function as ion-blocking electrodes. Recording EIS to very low frequencies (10 mHz) ensured capturing the electronic conduction process, free of any contribution from ionic conduction. Nevertheless, for NMC-PC at 25 °C, the ionic conductivity could not be discerned from the spectra even at high frequencies (1 MHz). The NMC-SC spectra, however, displayed the end of a semicircle, indicating that there was a significant contribution from ionic conductivity as well (**Figure 3b**). Hence, the respective equivalent circuits shown in **Figure 3**, with an electronic resistance ($R_e$) either in series with an inductor (I) or in parallel with an ionic resistor ($R_i$) and a constant phase element (CPE), were fitted to the spectra.

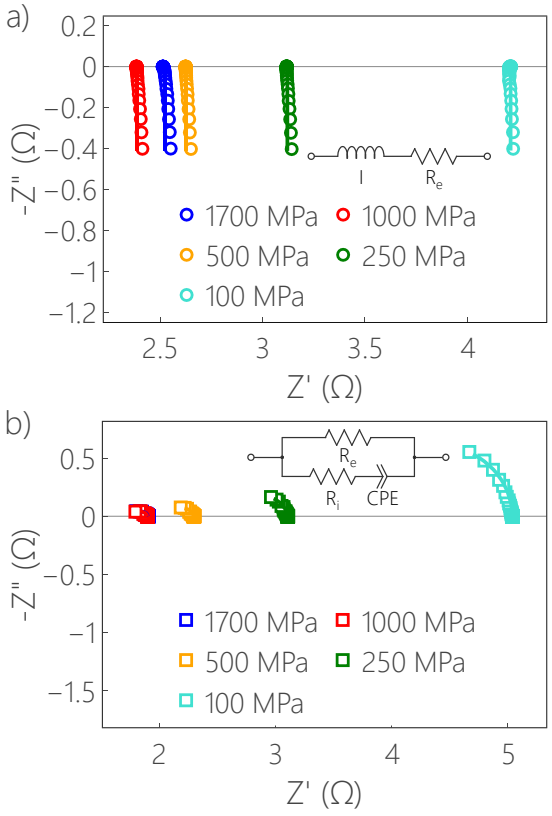


***Figure 3.*** *EIS spectra of a) NMC-PC and b) NMC-SC in the pelletized state, measured at various applied pressures (25 °C). The lines indicate fits to the equivalent circuits shown.*

The electronic resistivity during the initial powder compaction and the following pressure release could be calculated from the EIS fits (**Figure 4**). Note that the pressure dependence of the pellet thickness is often (incorrectly) ignored when conductivity values are reported in literature, instead using the pellet thickness measured without load. *In situ* thickness measurements under load are necessary to calculate the actual conductivity or resistivity with applied pressure, especially during the powder compaction step when the sample deformation is substantial (**Figure 2**).

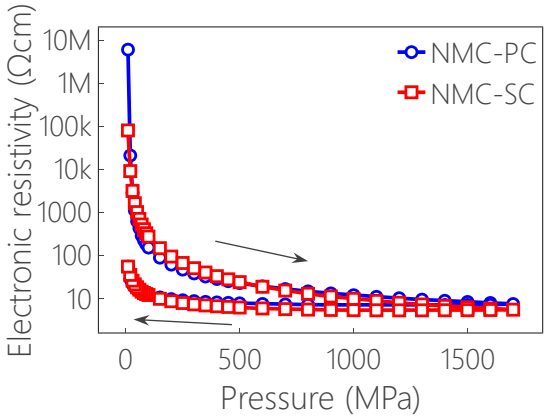


***Figure 4.*** *Electronic resistivity during the first pressure cycle. The pressure increase sweep corresponds to the initial powder densification.*

As seen in **Figure 4**, the electronic resistivity decreased by 4 – 6 orders of magnitude during the initial compaction step, as the powder was consolidated into a dense pellet. When the pressure was released, the resistivity remained more or less constant, and at 1 GPa the electronic conductivity was 145 mS/cm for NMC-PC and 191 mS/cm for NMC-SC, while the ionic conductivity of NMC-SC was 14 mS/cm. These relatively high conductivity values [3] are the result of the high pressure. At lower pressures, the conductivity decreased due to worsening electrical contact between grains.

When the temperature was decreased, the high-frequency portion of the NMC-PC spectra transitioned from pure inductance to a more sloping feature and finally a flat semicircle (**Figure 5a**). This indicates that the ionic conductivity became slow enough to be visible in the recorded frequency range. Therefore, the modified equivalent circuit shown in **Figure 5a** was used for the NMC-PC spectra at ≤10 °C, to fit also the

ionic resistance. For NMC-SC, both processes were visible in the spectra at all recorded temperatures (-30 – 100 °C, **Figure 5b**).

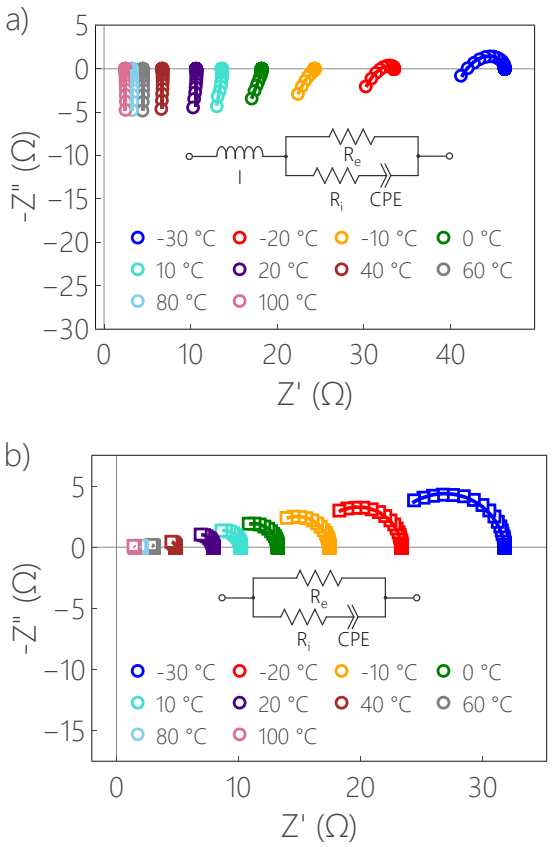


***Figure 5.*** *EIS spectra of a) NMC-PC and b) NMC-SC at various temperatures (200 MPa). The lines indicate equivalent circuit fits.*

Since the contribution from the ionic conductivity was more visible at low temperatures, the pressure ramp was repeated at -30 °C (**Figure 6**). The electronic conductivity increased with pressure, and there was significant hysteresis between the pressure increase and decrease. This follows the improved grain/grain and electrode/grain electrical contact as the sample is pressed. The ionic conductivity, on the other hand, generally decreased with pressure in the range 30 – 1000 MPa. This is analogous to the behaviour of some solid-state electrolytes, where the crystal lattice deforms under increased pressure, making ion diffusion more difficult [10, 11]. This trend reversed at the lowest pressures (<30 MPa), however, as the electrode contact resistance became significant.

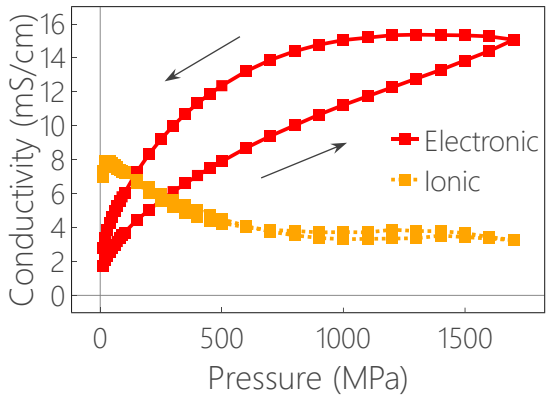


***Figure 6.*** *Ionic and electronic conductivity of the pressed NMC-SC pellet at -30 °C.*

The ionic and electronic conductivities at various temperatures are shown in the Arrhenius plot in **Figure 7**. All conductivities followed the Arrhenius equation in this temperature range. The activation energies for the conduction of ions and electrons in these two CAM samples are shown in **Table 1**. The activation energy for electron conduction was 0.18 eV for both samples, which is rather low for NMC, as expected for this high nickel content [3]. The activation energy for ion conduction was much larger for NMC-PC than for NMC-SC, hinting at a significant energy barrier for ion diffusion across grain boundaries, which is more prominent in polycrystalline materials with

small crystallites. Ions in single crystal samples, on the other hand, can travel further within the larger crystallites without being impeded by grain boundaries.

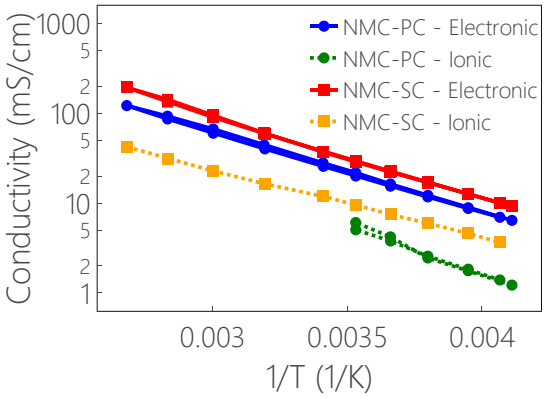


***Figure 7.*** *Arrhenius plot of the electronic (solid lines) and ionic (dotted lines) conductivity (200 MPa).*

***Table 1.*** *Activation energies (eV) for the conduction of electrons and ions in NMC-PC and NMC-SC.*

| $E_a$ (eV) | Electron | Ion |
|---|---|---|
| NMC-PC | 0.18 | 0.23 |
| NMC-SC | 0.18 | 0.15 |

# Summary

The mechanical and electrical properties of two pristine samples of high-nickel content NMC were measured at various pressures and temperatures. The densification process of the pure CAM powders was monitored by measuring the density using the *in-situ* determined sample thickness at various pressures, as well as determining the decreasing electronic resistivity as the materials were pressed. Furthermore, the electronic and ionic conductivity of the pressed materials could be separated by EIS. While the electronic conductivity increased with pressure, the ionic conductivity exhibited the opposite behaviour. Finally, the temperature dependence of these two charge transport processes allowed for the determination of their respective activation energies.

This detailed characterization was made possible by the use of a CompreDrive applying precise pressure and temperature setpoints to a CompreCell equipped with LVDT sensors for sample thickness monitoring. The same setup is also ideal for anode active materials, as well as for active material composites including binder, conductive additives, and a mixture of several active materials, to systematically investigate the influence of electrode composition.

# Acknowledgement

This study was performed in collaboration with BASF. Dr. Holger Schneider (BASF SE) is greatly acknowledged for the productive discussions and for enabling the use of the CAM samples in this application note.

# Literature

[1] B. Lu, Y. Yuan, Y. Bao, Y. Zhao, Y. Song and J. Zhang, "Mechanics-based design of lithium-ion batteries: a perspective," *Physical Chemistry Chemical Physics,* vol. 24, no. 48, pp. 29279-29297, 2022.

[2] R. Ruess, S. Schweidler, H. Hemmelmann, G. Conforto, A. Bielefeld, D. A. Weber, J. Sann, M. T. Elm and J. Janek, "Influence of NCM Particle Cracking on Kinetics of Lithium-Ion Batteries with Liquid or Solid Electrolyte," *Journal of The Electrochemical Society*, vol. 167, p. 100532, 2020.

[3] S. Wang, M. Yan, Y. Li, C. Vinado and J. Yang, "Separating electronic and ionic conductivity in mix-conducting layered lithium transition-metal oxides," *Journal of Power Sources*, vol. 393, pp. 75-82, 2018.

[4] rhd instruments GmbH & Co. KG, "CompreCell 6/12," [Online]. Available: https://rhd-instruments.de/solutions-and-products/for-solid-state-batteries/comprecell-12/.

[5] rhd instruments GmbH & Co. KG, "LVDT Distance Add-on," [Online]. Available: https://rhd-instruments.de/solutions-and-products/for-solid-state-batteries/lvdt-distance-add-on/.

[6] rhd instruments GmbH & Co. KG, "CompreDrive," [Online]. Available: https://rhd-instruments.de/solutions-and-products/for-solid-state-batteries/compredrive/.

[7] rhd instruments GmbH & Co. KG, "HC-Addon," [Online]. Available: https://rhd-instruments.de/solutions-and-products/for-solid-state-batteries/hc-addon/.

[8] rhd instruments GmbH & Co. KG, "Edelweiss," [Online]. Available: https://rhd-instruments.de/solutions-and-products/for-data-treatment-and-plotting/edelweiss/.

[9] rhd instruments GmbH & Co. KG, "RelaxIS," [Online]. Available: https://rhd-instruments.de/solutions-and-products/for-eis-data-analysis/relaxis/.

[10] V. Faka, M. Alabdali, M. A. Lange, F. M. Zanotto, C. Yildirim, M. D. Kanedal, J. Kondek, M. Hartmann, O. Maus, D. Daisenberger, M. R. Hansen, J. Keckes, D. Rettenwander, A. A. Franco and W. G. Zeier, "How Particle Size Affects Consolidation Behavior, Strain and Properties of Li6PS5Cl Fast Ionic Conductors," *Advanced Energy Materials*, p. e05186, 2026.

[11] "Application note: All-Solid-State Battery Testing up to 407 MPa using the CompreFrame," October 2025. [Online]. Available: https://rhd-instruments.de/magazine/all-solid-state-battery-testing-up-to-407-mpa-using-the-compreframe/.